

Exterior complex scaling method in TDDFT: HHG of Ar atoms in intense laser fields

K E Sosnova¹, D A Telnov¹, E B Rozenbaum¹ and S I Chu²

¹ Department of Physics, St. Petersburg State University, St. Petersburg 198504, Russia

² Department of Chemistry, University of Kansas, Lawrence, Kansas 66045, USA

E-mail: k.sosnova@pcqnt1.phys.spbu.ru

Abstract. The exterior complex scaling (ECS) method is applied in the framework of time-dependent density-functional theory (TDDFT) to study high-order harmonic generation (HHG) of multielectron atoms in intense laser fields. With the help of ECS, correct outgoing-wave boundary conditions can be imposed on the wave functions at large distances. In our implementation, ECS is combined with the time-dependent generalized pseudospectral method for accurate and efficient solution of the time-dependent Kohn-Sham equations. We make use of LB94 exchange-correlation potential which appears quite accurate in calculations of unperturbed electronic structure of Ar. Calculations of HHG are performed for the laser fields with the wavelength of 800 nm and several peak intensities. The HHG spectrum exhibits an intensity-independent minimum corresponding to the photon energy of about 51 eV which is closely related to the Cooper minimum in the photoionization cross section of Ar. We found that HHG spectra calculated with the frozen-core potential (not including dynamic response of the electron density) differ significantly from those obtained by TDDFT.

1. Introduction

Atomic systems subject to laser fields can be ionized. At large distances from the core, the wave function should contain only outgoing-wave components (describing ionization). Thus the correct boundary conditions are the outgoing-wave boundary conditions, if ionization takes place. We can impose these boundary conditions using an absorbing layer placed at some distance from the core. It prevents the electron density from moving back to the core thus imposing the correct boundary conditions. However, the properties of the absorber may influence the results (high-order harmonics spectra, for example).

The correct boundary conditions can be imposed in another way by performing a complex-scaling transformation [1, 2]. The complex-scaled wave function is supposed to vanish at infinity in the coordinate space, that gives the unscaled wave function satisfying the outgoing-wave boundary conditions. Uniform complex scaling, however, is not suited for time-dependent problems since the external field changes sign twice per optical cycle. Thus the complex-scaled propagator may diverge at large distances. The problem can be solved by exterior complex scaling. Dipole interaction with external field can be applied in the interior (not complex-scaled) domain only, and we choose it large enough to include all physically important regions.

Exterior complex scaling (ECS) [3, 4] may have advantages when applied to more complex systems described by potentials with non-analytical behaviour (or defined only numerically) in the interior region of the coordinates. The ECS method implies that the coordinate space is split in two domains, and only exterior domain is subject to the complex scaling transformation, while in the interior domain the wave function remains unchanged. The ECS mapping function may have continuous or discontinuous



derivative on the boundary between the two regions; these two cases are termed smooth ECS and sharp ECS, respectively.

In this paper, we briefly discuss an implementation of ECS in the framework of the time-dependent density functional theory (TDDFT) and its application to the calculations of the high-order harmonic generation (HHG) of Ar atoms in intense laser fields. A more detailed analysis of the Ar HHG spectra as well as discussion of the accompanying process of multiphoton ionization can be found in our recent article [5].

2. Smooth ECS

For solving the time-dependent and time-independent Schrödinger or Kohn-Sham equations, we apply the generalized pseudospectral (GPS) discretization of wave functions and operators in spherical coordinates. The details of the GPS discretization can be found in [6, 7] for the case of two-center systems and prolate spheroidal coordinates.

We require the mapping function $r(x)$ along with its first and second derivatives to be continuous on the boundary between the domains and adopt the following mapping transformation:

$$r = r(x), \quad r(x) = R(x) \exp[i\alpha(x)], \quad (1)$$

where $R(x)$ is a real monotonous function which maps the interval $[-1, 1]$ to the radial coordinate range $[0, R_b]$ used to solve the equations:

$$R(x) = R_m \frac{(1+x)^2 + 2\delta(1+x)}{1-x + 4R_m(1+\delta)/R_b}. \quad (2)$$

Here R_m , R_b , and δ are parameters of the transformation. The value of R_b must be large enough so all important physics can be included.

The phase $\alpha(x)$ characterizes the complex rotation of the radial coordinate in Eq. (1). We use the following piecewise polynomial dependence of α on x :

$$\alpha(x) = \begin{cases} 0, & -1 \leq x \leq x_0; \\ 10\alpha_0 \frac{(x-x_0)^5}{(x_1-x_0)^5} \left[\frac{(x_1-x)^2}{(x-x_0)^2} + \frac{1}{2} \frac{(x_1-x)}{(x-x_0)} + \frac{1}{10} \right], & x_0 \leq x \leq x_1; \\ \alpha_0, & x_1 \leq x \leq 1. \end{cases} \quad (3)$$

In the interior domain, $x < x_0$, $\alpha(x) = 0$; within the range $[x_0, x_1]$, $\alpha(x)$ gradually increases to reach the value α_0 at $x = x_1$; in the asymptotic region, $x > x_1$, the complex rotation angle is equal to α_0 .

In the coordinate space, the radius of the interior domain, $R(x_0)$, should be sufficiently large to accommodate oscillations in the laser field of a free electron emerging in the vicinity of the nucleus.

3. Electronic structure calculations of argon atoms

First, we solve the set of time-independent Kohn-Sham equations for the unperturbed spin orbitals $\psi_{n\sigma}(\mathbf{r})$ and spin orbital energies $\epsilon_{n\sigma}$:

$$\left[-\frac{1}{2}\nabla^2 + V_\sigma^s(\mathbf{r}) \right] \psi_{n\sigma}(\mathbf{r}) = \epsilon_{n\sigma} \psi_{n\sigma}(\mathbf{r}), \quad (4)$$

$$n = 1, 2, \dots, N_\sigma.$$

Here $N_\sigma (= N_\uparrow \text{ or } N_\downarrow)$ is the total number of electrons for a given spin σ ; the total number of electrons in the system is $N = N_\uparrow + N_\downarrow$. The electron spin densities $\rho_\sigma(\mathbf{r})$ and the total density $\rho(\mathbf{r})$ are related to the spin orbitals as follows:

$$\rho_\sigma(\mathbf{r}) = \sum_{n=1}^{N_\sigma} |\psi_{n\sigma}(\mathbf{r})|^2, \quad \rho(\mathbf{r}) = \rho_\uparrow(\mathbf{r}) + \rho_\downarrow(\mathbf{r}), \quad (5)$$

and the effective single-particle potential $V_{\sigma}^s(\mathbf{r})$ can be written down as a sum of three different terms:

$$V_{\sigma}^s(\mathbf{r}) = v_n(\mathbf{r}) + v_H(\mathbf{r}) + v_{xc,\sigma}(\mathbf{r}). \quad (6)$$

Here $v_n(\mathbf{r})$ is a Coulomb interaction of the electron with the nucleus (with $Z = 18$ being the nuclear charge of Ar) and $v_H(\mathbf{r})$ is the Hartree potential due to electron-electron repulsion:

$$v_n(\mathbf{r}) = -\frac{Z}{r}, \quad v_H(\mathbf{r}) = \int \frac{\rho(\mathbf{r}')d^3r'}{|\mathbf{r}-\mathbf{r}'|}. \quad (7)$$

The remaining term $v_{xc,\sigma}(\mathbf{r})$ is the exchange-correlation potential. Its exact expression is unknown but high-quality approximations are becoming available. For example, in this work we apply the exchange-correlation potential LB94 by van Leeuwen and Baerends [8]. Since Ar is a closed-shell atom, the electron densities for spin up and spin down are the same, hence the set of equations (4) must be solved for only one spin projection (either spin up or spin down). The equations are solved self-consistently, starting from some reasonable approximation for the potential $V_{\sigma}^s(\mathbf{r})$, until convergence is achieved.

4. TDDFT-ECS calculations for argon atoms

For the atoms subject to external time-dependent fields, we use TDDFT and solve the set of *time-dependent* Kohn-Sham equations:

$$i\frac{\partial}{\partial t}\psi_{n\sigma}(\mathbf{r},t) = H(t)\psi_{n\sigma}(\mathbf{r},t), \quad n = 1, 2, \dots, N_{\sigma}; \quad (8)$$

$$H(t) = -\frac{1}{2}\nabla^2 + V_{\sigma}^s(\mathbf{r},t) + v_{\text{ext}}(\mathbf{r},t). \quad (9)$$

The potential $v_{\text{ext}}(\mathbf{r},t)$ in Eq. (9) describes the interaction with the laser field. Taking into account the dipole approximation and the length gauge, one obtains it in the following form:

$$v_{\text{ext}}(\mathbf{r},t) = \mathbf{F}(t) \cdot \mathbf{r}. \quad (10)$$

Here $\mathbf{F}(t)$ is the electric field strength of the laser field, and the linear polarization is assumed. In this study, we use the laser pulses with the sine-squared envelope:

$$\mathbf{F}(t) = \mathbf{F}_0 \sin^2 \frac{\pi t}{T} \sin \omega_0 t, \quad (11)$$

where T and ω_0 denote the pulse duration and the carrier frequency, respectively; F_0 is the peak field strength. In all our calculations, we use the laser wavelength 800 nm ($\omega_0 = 0.056954$ a.u.) and the pulse duration of 20 optical cycles (full width at half maximum is about 27 fs).

For TDDFT energy functional, we adopt the adiabatic approximation. That means the time-dependent single-particle potential $V_{\sigma}^s(\mathbf{r},t)$ is defined by the same expression (6) as in the time-independent case but using the time-dependent electron densities. The initial values ($t = 0$) of Kohn-Sham spin orbitals and unperturbed (field-free) Hamiltonian are taken from the solution of Eq. (4). We represent the total Hamiltonian of Eq. (9) as a sum of the unperturbed Hamiltonian H_0 and interaction term $V(t)$ due to the external field:

$$H(t) = H_0 + V(t), \quad (12)$$

$$H_0 = -\frac{1}{2}\nabla^2 + V_{\sigma}^s(\mathbf{r},0), \quad (13)$$

$$V(t) = V_{\sigma}^s(\mathbf{r},t) - V_{\sigma}^s(\mathbf{r},0) + v_{\text{ext}}(\mathbf{r},t). \quad (14)$$

To propagate the Kohn-Sham spin orbitals in time, we use the second-order split-operator formula for the short-term propagator $U(t, \Delta t)$ at each time step:

$$U(t, \Delta t) = \exp \left[-i \frac{1}{2} \Delta t H_0 \right] \exp \left[-i \Delta t V \left(t + \frac{1}{2} \Delta t \right) \right] \exp \left[-i \frac{1}{2} \Delta t H_0 \right]. \quad (15)$$

Here the field-free propagator $\exp \left[-i \frac{1}{2} \Delta t H_0 \right]$ is *time-independent* and calculated only once using the spectral expansion:

$$\exp \left[-i \frac{1}{2} \Delta t H_0 \right] = \sum_k \exp \left[-i \frac{1}{2} \Delta t E_k \right] |\psi_k^R\rangle \langle \psi_k^L| \quad (16)$$

where E_k are the complex eigenvalues of the *non-Hermitian* ECS Hamiltonian H_0 . The right eigenvectors ψ_k^R and left eigenvectors ψ_k^L are subject to biorthogonality and normalization condition:

$$\langle \psi_k^L | \psi_{k'}^R \rangle = \delta_{kk'}. \quad (17)$$

The external field propagator $\exp \left[-i \Delta t V \left(t + \frac{1}{2} \Delta t \right) \right]$ is time dependent and must be calculated at each time step; however, upon GPS discretization it is represented by a diagonal matrix, thus its computation is fast enough. To avoid numerical instabilities related to the complex-scaled long-range dipole term, the interaction with the external field $V(t)$ in the propagator is restricted to the interior domain only.

5. High-order harmonic generation of argon atoms

To calculate the HHG spectra, we use a semiclassical approach, where the basic expressions come from the classical electrodynamics but the classical quantities such as dipole moment and its acceleration are replaced with the corresponding quantum expectation values. Using the Fourier transforms of the acceleration $\mathbf{a}(t)$ or dipole moment $\mathbf{d}(t)$, we can express the spectral density of radiation energy as follows [9]:

$$S(\omega) = \frac{2}{3\pi c^3} |\tilde{\mathbf{a}}(\omega)|^2 = \frac{2\omega^4}{3\pi c^3} |\tilde{\mathbf{d}}(\omega)|^2; \quad (18)$$

$$\tilde{\mathbf{a}}(\omega) = \int_{-\infty}^{\infty} dt \mathbf{a}(t) \exp(i\omega t), \quad (19)$$

$$\tilde{\mathbf{d}}(\omega) = \int_{-\infty}^{\infty} dt \mathbf{d}(t) \exp(i\omega t), \quad (20)$$

(c is the speed of light) and the expectation values of the dipole moment and acceleration are defined according to the following equations:

$$\mathbf{d}(t) = \int d^3r \mathbf{r} \rho(\mathbf{r}, t), \quad (21)$$

$$\mathbf{a}(t) = - \int d^3r \nabla [v_n(\mathbf{r}) + v_{\text{ext}}(\mathbf{r}, t)] \rho(\mathbf{r}, t). \quad (22)$$

They satisfy the same relation as the corresponding classical quantities:

$$\frac{d^2}{dt^2} \mathbf{d}(t) = \mathbf{a}(t). \quad (23)$$

The expression for $\mathbf{a}(t)$ can be obtained from that for $\mathbf{d}(t)$ with the help of the Ehrenfest theorem. For the expectation value of acceleration, the spatial integration in Eq. (22) emphasizes short distances; for the expectation value of dipole moment, Eq. (21), the spatial integration emphasizes long distances. In our calculations of the HHG spectra, we use the acceleration form; it is regarded to be more accurate since our numerical wave functions are of better quality at short distances due to denser spatial grid.

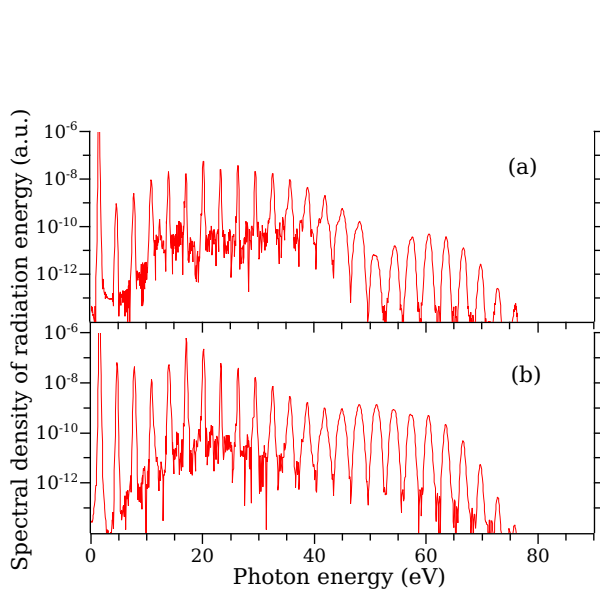


Figure 1. Spectral density of harmonic radiation energy for a \sin^2 laser pulse with carrier wavelength of 800 nm and duration of 20 optical cycles at the peak intensity 2×10^{14} W/cm²: (a) TDDFT results; (b) frozen-core model potential calculations.

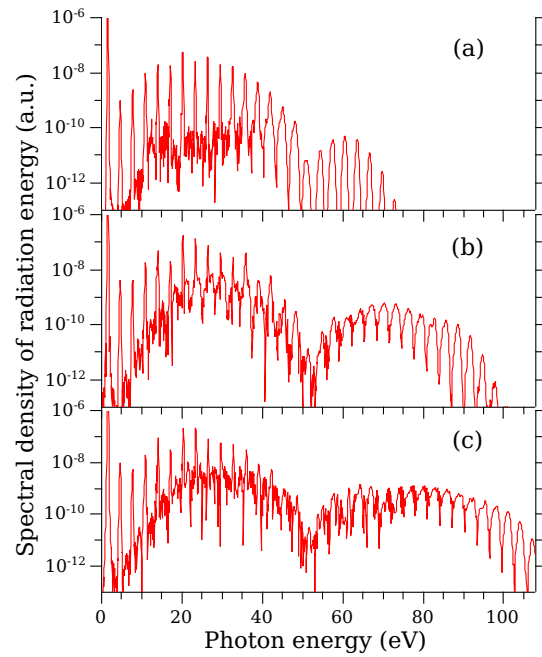


Figure 2. Spectral density of harmonic radiation energy for a \sin^2 laser pulse with carrier wavelength of 800 nm and duration of 20 optical cycles at the peak intensity: (a), 2×10^{14} W/cm²; (b), 3×10^{14} W/cm²; (c), 4×10^{14} W/cm².

In Fig. 1, we present the HHG spectra for the laser peak intensity 2×10^{14} W/cm²; the upper panel contains the TDDFT spectrum, while on the lower panel the results of the frozen-core model potential calculations are shown. Both frozen-core model and TDDFT spectra have a minimum in the central part which is closely related to the Cooper minimum [10] observed in the photoionization cross sections of Ar. This minimum is due to the nodal structure of the $3p$ wave function of Ar which causes the bound-continuum $3p - Ed$ dipole matrix element to vanish at some energy E in the continuum [10]. According to the three-step model of HHG [11], the third step of this process is recombination of the recolliding electron with the core. Ionization and recombination are mutually inverse processes, hence a minimum in the photoionization cross section must manifest itself in the HHG spectra as well. The Cooper minimum in the HHG spectra of Ar has already been observed experimentally many times [12–16]. In our TDDFT calculations, this minimum is clearly seen in the vicinity of the 33rd harmonic (51 eV). The frozen-core model potential calculations give the minimum less pronounced and shifted to lower energies (about the 29th harmonic, 45 eV). We note that another one-electron model [17] also reveals this minimum at lower energies (40 eV). We can conclude that dynamic multielectron response is quite important in shaping the Cooper minimum in the Ar HHG spectra.

Fig. 2 shows the HHG spectra of Ar calculated by the TDDFT-ECS method at three different intensities: 2×10^{14} W/cm², 3×10^{14} W/cm², and 4×10^{14} W/cm². The well-known semiclassical law [18] ($E_{\text{cutoff}} = E_i + 3.17U_p$, E_i and U_p being the ionization energy and the ponderomotive potential, respectively) is satisfied as the cutoff of the HHG spectrum shifts to higher energies with increasing intensity. At the same time, the position of the Cooper minimum in the spectrum appears intensity independent and corresponds approximately to 51 eV (33rd harmonic), in good accord with the experimental observations [13–15] (51 – 54 eV). We also point out the importance of the multielectron

effects and dynamic core polarization which is clearly seen from the comparison of our TDDFT and frozen-core model calculations.

6. Summary

In this paper, the TDDFT-ECS method has been presented for treatment of multielectron atoms subject to laser fields. We have shown that exterior complex scaling can be successfully implemented in the framework of time-dependent density-functional theory. It ensures that the wave function satisfies the outgoing-wave boundary conditions at large distances and gives a correct description of ionization caused by external time-dependent fields. When combined with the generalized pseudospectral discretization, TDDFT-ECS method provides an accurate and efficient computational scheme for calculations of multiphoton processes in atomic and molecular systems. We have applied the method to calculate high-order harmonic generation in Ar. Our results show that it is very important to take into account dynamic multielectron response in this process. In the HHG spectra of Ar, the effect of multiple electronic shells is clearly seen in shaping of the Cooper minimum. In the TDDFT-ECS calculations, this minimum appears approximately at the photon energy of 51 eV, in good agreement with the experimental data, while in the frozen-core potential model the minimum is less pronounced and shifted to lower energies.

Acknowledgments

This work was partially supported by the Chemical Sciences, Geosciences and Biosciences Division of the Office of Basic Energy Sciences, Office of Sciences, US Department of Energy. We also acknowledge the partial support of St. Petersburg State University (Grant No. 11.38.654.2013).

References

- [1] Balslev E and Combes J M 1971 *Commun. Math. Phys.* **22** 280
- [2] Aguilar A and Combes J M 1971 *Commun. Math. Phys.* **22** 265
- [3] Nicolaides C A and Beck D R 1978 *Phys. Lett. A* **65** 11
- [4] Simon B 1979 *Phys. Lett. A* **71** 211
- [5] Telnov D A, Sosnova K E, Rozenbaum E and Chu S I 2013 *Phys. Rev. A* **87** 053406
- [6] Telnov D A and Chu S I 2005 *Phys. Rev. A* **71** 013408
- [7] Telnov D A and Chu S I 2007 *Phys. Rev. A* **76** 043412
- [8] van Leeuwen R and Baerends E J 1994 *Phys. Rev. A* **49** 2421
- [9] Landau L D and Lifshitz E M 1975 *The Classical Theory of Fields* (Oxford: Pergamon Press)
- [10] Cooper J W 1962 *Phys. Rev.* **128** 681
- [11] Lewenstein M, Balcou P, Ivanov M Y, L'Huillier A and Corkum P B 1994 *Phys. Rev. A* **49** 2117
- [12] Minemoto S, Umegaki T, Oguchi Y, Morishita T, Le A T, Watanabe S and Sakai H 2008 *Phys. Rev. A* **78** 061402(R)
- [13] Wörner H J, Niikura H, Bertrand J B, Corkum P B and Villeneuve D M 2009 *Phys. Rev. Lett.* **102** 103901
- [14] Farrell J P, Spector L S, McFarland B K, Bucksbaum P H and Gühr M 2011 *Phys. Rev. A* **83** 023420
- [15] Higuat J *et al* 2011 *Phys. Rev. A* **83** 053401
- [16] Wang X, Chini M, Zhang Q, Zhao K, Wu Y, Telnov D A, Chu S I and Chang Z 2012 *Phys. Rev. A* **86** 021802(R)
- [17] Le A T, Morishita T and Lin C D 2008 *Phys. Rev. A* **78** 023814
- [18] Corkum P B 1993 *Phys. Rev. Lett.* **71** 1994